BIOCHEMISTRY
including biophysical chemistry & molecular biology
Article

Biochemistry **2010,** *49,* 10647–10655 10647
DOI: 10.1021/bi101448t

Biochemical and Physiological Characterization of a BLUF Protein−EAL Protein Complex Involved in Blue Light-Dependent Degradation of Cyclic Diguanylate in the Purple Bacterium *Rhodopseudomonas palustris*[†]

Takuya Kanazawa,[‡] Shukun Ren,[§] Mikika Maekawa,[‡] Koji Hasegawa,[∥] Fumio Arisaka,[‡] Mamoru Hyodo,[⊥] Yoshihiro Hayakawa,[@] Hiroyuki Ohta,[§] and Shinji Masuda*[,§,#]

[‡]*Graduate School of Bioscience and Biotechnology, and* [§]*Center for Biological Resources and Informatics, Tokyo Institute of Technology, Yokohama 226-8501, Japan,* [∥]*Advancesoft Corporation, Akasaka, Tokyo 107-0052, Japan,* [⊥]*Graduate School of Pharmaceutical Sciences, Hokkaido University, Sapporo 060-0812, Japan,* [@]*Faculty of Engineering, Aichi Institute of Technology, Toyota 470-0392, Japan, and* [#]*PRESTO, Japan Science and Technology Agency, Saitama 332-0012, Japan*

Received September 7, 2010; Revised Manuscript Received November 1, 2010

ABSTRACT: Organisms adapt their physiologies in response to the quality and quantity of environmental light. Members of a recently identified photoreceptor protein family, BLUF domain proteins, use a flavin chromophore to sense blue light. Herein, we report that PapB, which contains a BLUF domain, controls the biofilm formation of the purple photosynthetic bacterium *Rhodopseudomonas palustris*. Purified PapB undergoes a typical BLUF-type photocycle, and light-excited PapB enhances the phosphodiesterase activity of the EAL domain protein, PapA, which degrades the second messenger, cyclic dimeric GMP (c-di-GMP). PapB directly interacts with PapA in vitro in a light-independent manner and induces a conformational change in the preformed PapA−PapB complex. A PapA−PapB docking simulation, as well as a site-directed mutagenesis study, identified amino acids partially responsible for the interaction between the PapA EAL domain and the two C-terminal α-helices of the PapB BLUF domain. Thus, the conformational change, which involves the C-terminal α-helices, transfers the flavin-sensed blue light signal to PapA. Deletion of *papB* in *R. palustris* enhances biofilm formation under high-intensity blue light conditions, indicating that PapB functions as a blue light sensor, which negatively regulates biofilm formation. These results demonstrate that *R. palustris* can control biofilm formation via a blue light-dependent modulation of its c-di-GMP level by the BLUF domain protein, PapB.

Microorganisms often adapt their physiologies to their environments. Cyclic dimeric GMP (c-di-GMP)[1] is a bacterial second messenger involved in certain complex physiological processes (*1*−*5*). It was first identified as an activator of cellulose synthase in *Acetobacter xylinum* (*6*). Later, it was shown to be ubiquitously present in bacteria and associated with cell motility, biofilm formation, virulence, and cell cycle progression (*1*−*4*, *7*−*11*). This second messenger is synthesized by diguanylate cyclases and is degraded by phosphodiesterases (*1*−*5*). Enzymes that catalyze the synthesis and hydrolysis of c-di-GMP contain the GGDEF (Gly-Gly-Asp-Glu-Phe) and EAL (Glu-Ala-Leu) domains, respectively (*1*−*5*, *12*−*16*). Several different c-di-GMP receptors have been identified, including the PilZ domain proteins (*9*−*11*, *17*, *18*). It was also found that c-di-GMP binds to a ribozyme class in mRNA for controlling gene expression (*19*−*22*). Despite the recent identification of enzymes responsible for c-di-GMP synthesis and hydrolysis, as well as the identification of the downstream components that respond to changes in c-di-GMP levels, how signal input proteins control cellular c-di-GMP levels is poorly understood. Interestingly, a GGDEF domain or an EAL domain often exists in the same protein as its corresponding sensory or regulatory domain, e.g., a light sensor domain (*1*−*5*).

Various blue light receptors are distributed among prokaryotes and eukaryotes (*23*, *24*). Sensors of blue light using flavin (BLUF) photoreceptors use a flavin chromophore to modulate many physiological activities in various microorganisms (*25*, *26*). A notable feature of BLUF domains is that they functionally interact with various output proteins. AppA, a BLUF domain protein from the purple bacterium *Rhodobacter sphaeroides*, modulates the DNA binding activity of the transcriptional factor PpsR to control photosynthesis gene expression (*27*−*29*). The cyanobacterial BLUF domain protein, PixD/Slr1694, interacts with the response regulator-like protein, PixE, to control phototaxis response (*30*−*32*). The *Escherichia coli* BLUF domain protein, YcgF, interacts with the MerR-like transcription factor, YcgE, to control biofilm formation in an extra-host environment (*33*−*35*). Biochemical analyses indicated that these interactions are light-dependent; each BLUF protein binds to its partner protein in the dark, and upon illumination, the complex dissociates (*27*, *34*, *36*). Thus, some BLUF proteins control various physiological processes by modulating the activities of transcription factors in a blue light-dependent fashion.

Several other BLUF protein families control the enzymatic activities of the output domains. Specifically, PAC from the green algae *Euglena gracilis* has two BLUF domains and two adenylate cyclase domains and requires blue light illumination for its

[†]This work was supported by the JST PRESTO program.

*To whom correspondence should be addressed. E-mail: shmasuda@bio.titech.ac.jp. Telephone: +81-45-924-5737. Fax: +81-45-924-5823.

[1]Abbreviations: c-di-GMP, cyclic dimeric GMP; l-di-GMP, linear dimeric GMP; BLUF, sensors of blue light using flavin; HPLC, high-performance liquid chromatography; FAD, flavin adenine dinucleotide; PCR, polymerase chain reaction; ORF, open reading frame; *c*, sedimentation coefficient; WT, wild type.

Published on Web 11/17/2010

adenylate cyclase activity (*37*). BlrP1 from *Klebsiella pneumoniae* has a BLUF domain and an EAL domain, and the latter's ability to hydrolyze c-di-GMP is induced by blue light (*38*). Thus, BLUF domains also function as light-sensing modules that activate an enzymatic domain in response to a blue light signal. However, how the signals are transferred from the BLUF domains to the output domains is not well understood.

Recently, blue light-dependent biofilm formation has been found in some nonphototrophic bacteria, such as *E. coli* (*34*), *Caulobacter crescentus* (*39*), and the deep sea bacterium *Idiomarina loihiensis* (*40*). Given the fact that these organisms live in very different environmental conditions, physiological meanings of the biofilm formation in response to blue light could differ among the bacteria, although the functions are not well understood. In the case of photosynthetic bacteria, control of blue light-dependent biofilm formation, if possible, may be complex, because they also need to sense light to control photosynthesis. However, blue light-dependent biofilm formation has not been found and characterized in any phototrophic bacteria.

For this study, we investigated some of the biochemical and physiological aspects of the blue light-controlled c-di-GMP degradation pathway that involves the BLUF domain protein, PapB, and the EAL domain protein, PapA, from the purple photosynthetic bacterium *Rhodopseudomonas palustris*. In response to blue light, PapB increased the c-di-GMP hydrolysis activity of PapA, which inhibited biofilm formation. Additionally, a light-induced intermolecular conformational change between the BLUF and EAL domains of these two proteins was necessary for c-di-GMP hydrolysis activity enhancement.

MATERIALS AND METHODS

Bacterial Strains and Growth Conditions. The *R. palustris* strain, CGA009, was the WT strain. This strain and its mutated forms, Δ*papA*, Δ*papB*, and Δ*papApapB*, were cultured in TYS medium containing 0.5% (w/v) bactotryptone, 0.1% (w/v) yeast extract, and 0.2% (w/v) disodium succinate. *E. coli* strains were cultured at 37 °C in Luria-Bertani medium. When appropriate, kanamycin was present at 100 mg/L in the *R. palustris* cultures. For the *E. coli* cultures, kanamycin was present at 50 mg/L and ampicillin was present at 100 mg/L.

Expression and Purification of R. palustris PapA and PapB. The nucleotide sequences of *R. palustris papA* and *papB* and the corresponding amino acid sequences for PapA (RPA0521) and PapB (RPA0522) were retrieved from the CyanoBase database at the KAZUSA DNA Research Institute website (http://genome.kazusa.or.jp/cyanobase/). Expression plasmids for His-tagged PapA and nontagged PapB were constructed as follows. The coding regions for PapA and PapB were PCR amplified using *R. palustris* genomic DNA as the template and the following primers: for *papA*, 5′-GGGGGGGCATATG-GGGGTAGTAGTCTCAGTCATC-3′ (*Nde*I) and 5′-GG-GAATTCGAGAGACTGACTTCCGTTGCC-3′ (*Eco*RI); and for *papB*, 5′-GGGGGGGCATATGCCGAGCGAGCTGTAT-CG-3′ (*Nde*I) and 5′-GGGAATTCTTAGGCGGCGCGGGC-TTCTTC-3′ (*Eco*RI). The underlined sequences lead to restriction sites in the PCR products. Amplified DNA fragments for *papA* and *papB* were digested with *Nde*I and *Eco*RI, and the products were cloned into an *Nde*I- and *Eco*RI-digested pET28a vector (Merck) and a pTYB12 vector (New England Biolabs), respectively. The inserted DNA sequences were confirmed by sequencing, and the plasmids were named pETPapA and pTY-PapB, respectively. Expression plasmids for the two mutants, PapA L510A and PapB R130A, in which PapA Leu510 and PapB Arg130 were each replaced with Ala, were generated using standard PCR-mediated site-directed mutagenesis with pETPapA and pTYPapB as template DNAs and complementary primers that contained mismatches so that the codons for Leu and Arg were converted to ones for Ala. The plasmids were each transferred into *E. coli* BL21(DE3) cells, and the proteins were expressed after induction with isopropyl 1-thio-D-galactopyranoside (final concentration of 1 mM) at 16 °C. The His-tagged PapA was purified using His-bind resin (Merck), and PapB was purified using chitin beads (New England Biolabs) according to the manufacturer's instructions. We found that purified PapB binds different flavin molecules, including riboflavin, flavin mononucleotide, and FAD, so that before purification, cell-free extract was incubated with a large molar excess of FAD (Sigma), which results in replacement of the flavins to FAD as described previously (*41*). Purified His-tagged PapA was dialyzed against 10 mM Tris-HCl (pH 8.0) and 200 mM NaCl. Purified PapB was dialyzed against 10 mM Tris-HCl (pH 8.0) and 5 mM NaCl. For concentration measurements, the absorption at 280 nm and a molar extinction coefficient of 41500 cm^{-1}, determined from its amino acid sequence, were used for PapA, and the absorbance of the flavin chromophore at 450 nm and a molar extinction coefficient of 11300 cm^{-1} were used for PapB.

Phosphodiesterase Assay. c-di-GMP was synthesized as described previously (*42*). For the c-di-GMP phosphodiesterase activity assay, solutions that contained 50 mM Tris-HCl (pH 8.0), 10 mM $MgCl_2$, 0.5 mM ethylenediaminetetraacetic acid, 50 mM NaCl, and 100 μM c-di-GMP with or without 3.2 μM purified PapB were used. The reactions were started by the addition of purified PapA (final concentration of 1.6 μM). The reaction mixtures were incubated at room temperature in the dark or under a halogen lamp (~900 μmol m^{-2} s^{-1}). After 0, 20, 60, and 120 min, 100 μL samples were withdrawn from the reaction mixtures. To terminate a reaction, 10 μL of 100 μM $CaCl_2$ was added to the reaction mixture, which was then boiled for 2 min. After centrifugation at 15000*g* for 10 min, the supernatants were filtered through SUPREC-01 (TaKaRa), and the eluates were analyzed by HPLC (Hitachi). The mixtures were each separated over a Supelcosil LC-18-T column [150 mm × 4.6 mm (Supelco)] with the gradient program described previously (*16*). Nucleotide absorbance was detected at 254 nm.

Analytical Ultracentrifugation. Sedimentation velocity experiments were performed with an Optima XL-I analytical ultracentrifuge (Beckman-Coulter) and an eight-hole An-50Ti rotor at 40000 rpm and 20 °C in a buffer containing 10 mM Tris-HCl (pH 8.0) and 40 mM NaCl. Moving boundary absorbances were recorded at 280 nm without delays between successive scans. The distribution of sedimentation coefficient $c(S)$ was obtained using SEDFIT (*43*), and subsequently, $c(S)$ was converted into the distribution of molecular weight $c(M)$ assuming that the frictional ratio, f/f_0, is common to all the molecular species present in solution (*43*).

In Vitro Pull-Down Assay. The pull-down assay was performed as described previously (*36*). Briefly, purified His-tagged PapA (50 μg) was incubated with His-bind resin (Merck) for 10 min in 10 mM Tris-HCl (pH 7.5) and 100 mM NaCl. The resin was poured into a column, and then a solution of purified PapB (50 μM) was cycled through the column five times in the absence or presence of light (900 μmol m^{-2} s^{-1}). After the resin had been washed twice with the same buffer, the recovered

proteins were subjected to sodium dodecyl sulfate−polyacrylamide gel electrophoresis (SDS−PAGE).

Construction of the R. palustris Mutated Strains, ΔpapA, ΔpapB, and ΔpapApapB. The *R. palustris papA*-disrupted strain, Δ*papA*, was constructed as follows. The DNA fragment that included *papA* and the 500 up- and downstream base pairs was PCR-amplified using genomic DNA as the template and the sets of primer pairs 5′-GGTTCGAGCTCATGGGGGTAG-TCTCAGTC-3′ (primer 1) and 5′-CGGGATCCAAACTCAT-CAGCCTCGATC-3′ (primer 2), and 5′-CGGGATCCGGGC-TTCGAGGCGCTGC-3′ (primer 3) and 5′-GCTCTAGATCA-GAGACTGACTTCCGTTG-3′ (primer 4), for the up- and downstream regions, respectively. The two PCR products were digested with *Sac*I and *Xba*I and then cloned into a *Sac*I- and *Xba*I-digested pZJD29A vector (*44*). The plasmid was digested with *Bam*HI, and the 1.5 kb *Bam*HI-digested kanamycin-resistant cassette from pBSL86 (*45*) was inserted into the *Bam*HI site. This plasmid was transferred into *R. palustris* cells by conjugation with the mobilizing strain S17-1 lysogenized with *λpir* (*46*). Kanamycin-resistant colonies found on plated agar that contained 5% sucrose were selected as double-crossover candidates, and the chromosomal insertion was confirmed by PCR. The *R. palustris papB*-disrupted strain, Δ*papB*, was constructed as follows. The DNA fragment that included *papB* and the 500 up- and downstream base pairs was PCR amplified using genomic DNA as the template and the primer pairs 5′-GGGCCGAGCTC-GGGCTTCGAGGCGCTGC-3′ (primer 5) and 5′-CGGGATC-CGGTCAGAGACTGACTTCCGTTG-3′ (primer 6), and 5′-CGGGATCCTATCGCTGCGTGTACTAC-3′ (primer 7) and 5′-GCTCTAGATTAGGCGGCGCGGGCTTC-3′ (primer 8), for the up- and downstream regions, respectively. The two PCR products were digested with *Sac*I and *Xba*I and then cloned into a *Sac*I- and *Xba*I-digested pZJD29A vector (*44*). Other procedures were the same as those used to construct Δ*papA* as described above. The *R. palustris papA*/*papB*-disrupted strain, Δ*papApapB*, was constructed as follows. The DNA fragment that included *papA*, *papB*, the 500 bp region upstream of *papA*, and the 500 bp region downstream of *papB* was PCR amplified using genomic DNA as the template. The primers used for the up- and downstream base pairs were primers 1 and 2 and primers 7 and 8, respectively. The two PCR products were digested with *Sac*I and *Xba*I and then cloned into a *Sac*I- and *Xba*I-digested pZJD29A vector (*44*). Other procedures were the same as those used to construct Δ*papA* as described above.

Biofilm Formation Assay. *R. palustris* strains that had been cultured to stationary phase were subcultured in 3 mL of fresh medium (30-fold dilution) and grown statically for 70 h in the dark or under a light-emitting diode [blue light, $\lambda_{max} = 470$ nm (Sanyo)] at an intensity of 50 μmol m^{-2} s^{-1} (low blue light) or 250 μmol m^{-2} s^{-1} (high blue light). Biofilms were visualized after the slow addition of 0.1% crystal violet (1 mL) (Wako), after incubation for 1 h, and after being washed with deionized water. The staining was quantified via addition of 2 mL of ethanol, vigorous mixing, and then measurement of the absorbance at 600 nm. The value for WT grown in the dark was set to 1.0 in each measurement, and the experiment was performed four times.

Binding Model for PapB and the EAL Domain in PapA. A PapB structure that contained a flavin mononucleotide was constructed using the coordinates of the *K. pneumoniae* BlrP1 X-ray structure (2.05 Å resolution; Protein Data Bank entry 3GFZ) by homology modeling. The BLUF domain of BlrP1 (residues 1−142) was used as the structural template for the PapB model. Sequence alignment of PapB (residues 4−147) with the BlrP1 BLUF domain was performed using ClustalW2 (*47*) (Figure 3 of the Supporting Information). The atomic coordinates of the flavin mononucleotide in the BLUF domain of BlrP1 were included during the modeling procedure. The PapB model was built with Homology Modeling for HyperChem (*48*). Similarly, the homology model for the monomeric EAL domain of PapA (residues 298−558) that contained c-di-GMP was constructed from the EAL domain of BlrP1 (residues 143−400). The PapA EAL homodimer was obtained by superposition of the Cα atoms of the two monomers onto the two EAL domains in the BlrP1 homodimer structure. The simulation for PapB docked into the PapA homodimer was performed using ZDOCK (*49*). A second PapB model was docked into the best PapB−$(PapA)_2$ structure using PapA dimer symmetry as a guide. All models were refined using the OPLS force field, and the qualities of the models were assessed using RAMPAGE (*50*) to confirm that the proper amino acid conformations existed.

RESULTS

PapA and PapB Activities. To investigate how BLUF domains control the activities of enzyme domains, we first searched for an ORF that specified a protein with a BLUF domain that could potentially interact with an enzymatic domain of a second protein. The *R. palustris* ORF, RPA0522, was chosen for this purpose. RPA0522 encodes a small single-domain protein (~16.5 kDa) with a sequence that is similar to those of BLUF domains. RPA0522 and ORF RPA0521 are part of the same operon (Figure 1 of the Supporting Information), which suggested that they may interact functionally (*25*). The primary structure of RPA0521 indicated that it is a multidomain protein (~61.8 kDa) with regions at its N- and C-termini that are similar in sequence to GGDEF and EAL domains, respectively. However, the two glycines that are part of GGDEF motifs are not conserved in RPA0521; the EADEF sequence is present instead. Conversely, the C-terminal EAL motif in RPA0521 is conserved. These observations suggested that RPA0521 functions as a c-di-GMP phosphodiesterase and that it does not have c-di-GMP synthase activity. We hypothesized that RPA0522, because it contains a BLUF domain, controls the enzymatic activity of RPA0521 in a blue light-dependent manner. We named the proteins PapA (RPA0521) and PapB (RPA0522) (photo-activated phosphodiesterase A and B, respectively).

Recombinant PapA and PapB were expressed in *E. coli* and were affinity purified. Figure 1A shows the UV−visible absorption spectra of purified PapB under dark and light conditions. The spectrum of dark-adapted PapB has two broad peaks, centered at 386 and 445 nm (Figure 1A, black line), which arise from the oxidized flavin chromophore and are very similar in shape to the spectra found for other BLUF proteins (*27*, *31*, *33*). PapB underwent a typical BLUF-type photocycle; the absorption spectrum shifted by ~10 nm to longer wavelengths upon light illumination (Figure 1A, red line). The PapB difference spectra (light − dark) are also very similar to those reported for other BLUF proteins (Figure 1B) (*27*, *31*, *33*). The kinetics indicated that the light-induced spectrum of PapB decayed to that of the dark state with simple first-order kinetics [Figure 2A (■)]. The half-time for the light-induced state at pH 8.0 was ~4 s, which is similar to that found for the BLUF protein PixD (~5 s) (*31*). These observations indicated that the spectral properties of PapB are those typical for BLUF proteins.

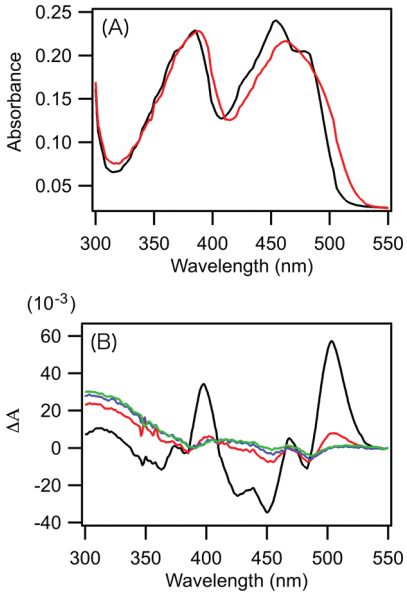

FIGURE 1: Spectral analysis of PapB. (A) UV−visible absorption spectra of dark-adapted (black) and light-adapted (red) PapB. (B) Difference spectra for PapB (light − dark). Spectra were recorded 0 (black), 5 (red), 10 (green), and 30 s (blue) after irradiation with white light (900 μmol m^{-2} s^{-1}).

We next examined the enzymatic activity of PapA. Purified PapA was mixed with c-di-GMP, and the reaction products were analyzed by HPLC. If PapA had a c-di-GMP-specific phosphodiesterase activity, the linear dimeric GMP (l-di-GMP) would be detected. As expected, the level of l-di-GMP increased with incubation time (Figure 3A), which indicated that PapA is a c-di-GMP-specific phosphodiesterase. We also assayed for c-di-GMP synthase activity. For this purpose, purified PapA was mixed with GTP, and the reaction products were analyzed. However, we did not detect c-di-GMP (Figure 3B). Thus, the PapA N-terminal GGDEF-like domain cannot catalyze the synthesis of c-di-GMP.

Recently, it was found that a GGDEF-like domain that lacks c-di-GMP synthase activity has a regulatory function (*51*). Specifically, the *C. crescentus* ORF, CC3396, contains a GEDEF sequence (instead of GGDEF) and binds GTP with a K_d of 4 μM. When GTP is bound, the C-terminal EAL domain of CC3396 is activated as a phosphodiesterase. Given these observations, we hypothesized that the PapA phosphodiesterase activity might be allosterically controlled in a similar manner by GTP, even though there are two amino acid substitutions in the GGDEF motif (changed to EADEF). We assayed for PapA phosphodiesterase activity in the presence of GTP. However, PapA was not activated by GTP; the specific phosphodiesterase activities (±standard error) of PapA in the absence and presence of 50 μM GTP are 0.40 ± 0.01 and 0.41 ± 0.01 nmol min^{-1} nmol^{-1}, respectively.

We next assayed for PapA phosphodiesterase activity in the presence of PapB. In the dark, the phosphodiesterase activity of PapA was not affected by PapB; the activity was identical to that found when PapB was not present (Table 1). However, in the light (~900 μmol m^{-2} s^{-1}), the PapA phosphodiesterase activity significantly increased (~2.5-fold) when PapB was present (Table 1). Thus, photoactivated PapB functioned as an enhancer for PapA phosphodiesterase activity.

A Direct Protein−Protein Interaction between PapA and PapB. Our phosphodiesterase assays indicated that PapB functionally interacted with PapA in a light-dependent manner.

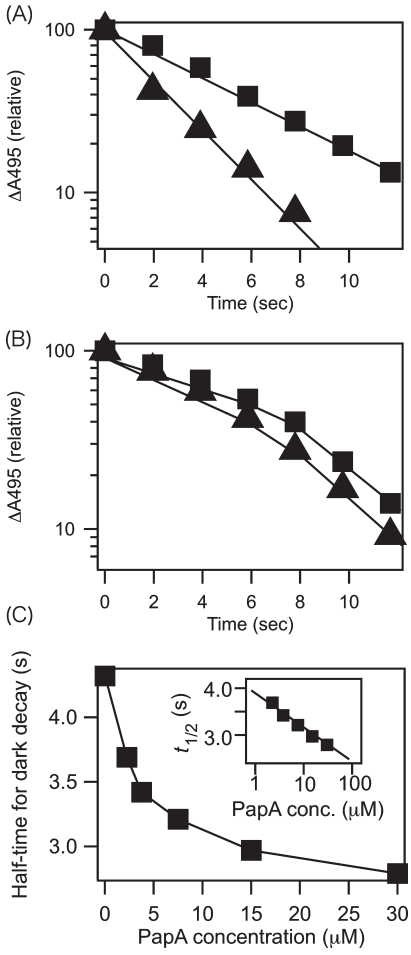

FIGURE 2: Decay kinetics of the light-induced absorption spectrum (recorded at 495 nm) of (A) WT PapB and (B) R130A. The proteins were dissolved in 10 mM Tris-HCl (pH 8.0) containing 68 mM NaCl. The kinetics were measured in the absence (■) and presence (▲) of PapA. (C) Half-times for dark decay of light state PapB were measured in the presence of different concentrations of PapA. The PapB concentration is 15 μM in each measurement. In the inset, the *X*-axis is in a logarithmic scale.

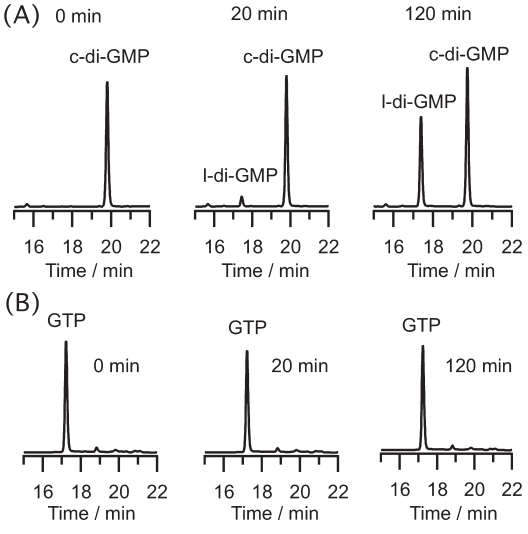

FIGURE 3: HPLC profiles showing (A) the hydrolysis of c-di-GMP by PapA and (B) the lack of c-di-GMP synthetic activity associated with PapA.

To better characterize the interaction, we determined the oligomerization status of the proteins. Analytical ultracentrifugation

Table 1: Effect of PapB on PapA Phosphodiesterase Activity[a]

condition	specific activity
PapA only (dark)	0.40 ± 0.01
PapA and PapB (dark)	0.41 ± 0.02
PapA and PapB (light)	1.01 ± 0.05

[a]The activities are reported as nanomoles of c-di-GMP hydrolyzed per minute per nanomole of protein. Light was provided by a halogen lamp with an intensity of ~900 μmol m^{-2} s^{-1}.

Table 2: $c(S)$ Values of Peaks[a] in the Analytical Ultracentrifugation Analysis of PapA, PapB, and the PapA−PapB Mixture

PapA:PapB ratio	peak 1	peak 2	peak 3
0.0:1.0	1.89	ND[b]	ND[b]
1.0:0.0	ND[b]	5.54	ND[b]
1.0:1.9	1.83	ND[b]	5.86
1.0:3.7	1.85	ND[b]	6.02
1.0:7.5	1.87	ND[b]	6.20

[a]Peaks 1, 2, and 3 are ascribed to the PapB monomer, the PapA dimer, and the reaction boundary of the PapA−PapB complex, respectively (for details, see the text). [b]Not detected.

analysis indicated that the sedimentation coefficient $c(S)$ values of PapA and PapB were 1.89 and 5.54, respectively (Table 2). The solution molecular masses of PapA and PapB were then calculated and determined to be 123.9 and 18.5 kDa, respectively (for details, see Materials and Methods). Given their amino acid sequences, the predicted molecular masses for PapA and PapB were 61.8 and 16.5 kDa, respectively. Thus, PapA existed as a dimer and PapB as a monomer. The analytical ultracentrifugation analysis was also performed with PapA in the presence of an excess of PapB (1.9−7.5-fold). As shown in Table 2, two distinct peaks were observed. One shows a $c(S)$ value (~1.85) almost identical to that observed for PapB only (1.89), suggesting that it is a peak for monomeric PapB. The other peak shows various $c(S)$ values (from 5.85 to 6.20) depending on the PapB concentration; higher $c(S)$ values could be seen with larger PapB:PapA ratios. This is a typical property for the reaction boundary of protein complexes that is observed when multimeric states are in fast equilibrium as compared with the time of experiment (*52*). Thus, the second peak (peak 3) is estimated to be a reaction boundary component of the PapA−PapB complex.

We next characterized the PapA−PapB interaction with a pull-down experiment using the purified proteins. For this assay, His-tagged PapA was bound to a Ni column, and then a solution of untagged PapB was passed through the column. After being washed, the proteins bound to the Ni column were eluted with buffer containing imidazole. When His-tagged PapA was not present, PapB did not bind to the column; conversely, when PapA was bound to the column, PapB was detected in the imidazole-containing eluate (Figure 4A, left), which indicated that PapB specifically interacted with PapA. The same experiment was also performed in the light [~900 μmol m^{-2} s^{-1} (Figure 4A, right)], and light did not significantly affect the interaction; PapB still bound to PapA on the column. Notably, the intensity of the light was the same as that used for the PapA phosphodiesterase assay, for which PapB enhanced PapA activity (Table 1).

Given that the interaction between PapA and PapB is light-independent, we considered whether the binding of PapA to PapB would influence the rate at which light-activated PapB

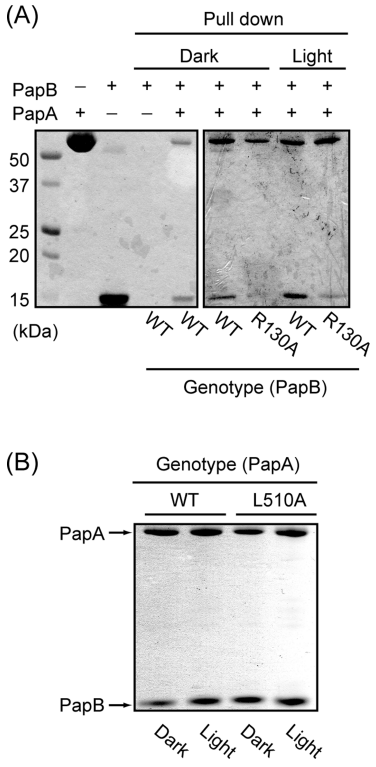

FIGURE 4: PapB interacts with PapA in a light-independent manner. (A) Pull-down assays that used His-tagged PapA and PapB or R130A. Purified WT PapB and R130A were each separately applied to a Ni column that contained bound His-tagged WT PapA. (B) Pull-down assays that used His-tagged PapA or L510A and PapB. Purified WT PapB was applied to Ni columns that contained bound WT PapA or L510A. For all assays, after the column had been washed, bound proteins were separated and identified by SDS−PAGE. The experiments were performed under dark and light conditions.

decayed to its dark state. We therefore measured the decay kinetics of the red-shifted PapB-bound flavin absorption in the presence of PapA. Although the absorption spectrum of PapB was not changed by the addition of PapA (data not shown), the decay kinetics of the red-shifted spectrum was significantly affected. Specifically, when an equimolar amount of PapA was mixed with PapB, the decay kinetics for light-activated PapB increased ~2-fold [Figure 2A (▲)], which indicated that, when PapA binds, a conformational change occurs in PapB that affects the structural dynamics of PapB. The half-time for the dark decay of the light-activated PapB (15 μM) was also measured at different concentrations of PapA (Figure 2C). The decay kinetics of PapB was clearly PapA-dependent, and the acceleration of the dark decay was nearly saturated with an equimolar amount of PapA (15 μM). Given that PapA and PapB exist as a monomer and dimer, respectively (Table 2), it is suggested that two PapB monomers bind to a PapA dimer.

We next performed a PapA−PapB docking simulation. To model the PapB (BLUF) and PapA (EAL) structures, we used the BlrP1 crystal structure as the template. BlrP1 is a homodimer, and each subunit contains a BLUF domain and an EAL domain (*38*). The BLUF domain of one BlrP1 subunit interacts with the EAL domain of the other subunit. We hypothesized that PapB might interact with PapA via the latter's EAL domain, because PapB directly controls the phosphodiesterase activity of PapA. For PapB (residues 4−147), the BlrP1 BLUF domain (residues 1−142) served as the template (*38*), and the obtained PapB structure has a typical BLUF domain fold, composed of an

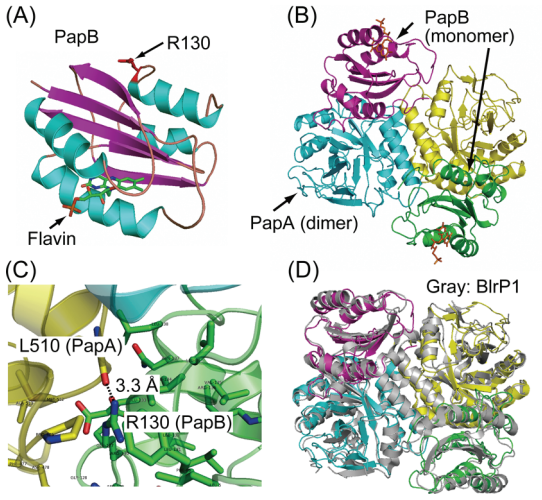

FIGURE 5: Homology modeling and a docking simulation. (A) The PapB model used the crystal structure of the BlrP1 BLUF domain as the template (*38*). The β-sheet is colored magenta, and the α-helices are colored blue. (B) Overall view of the docked PapA−PapB complex. The PapB monomers are colored magenta and green and the PapA monomers blue and yellow. (C) Positions of PapB R130 and PapA L510 in the docked complex. The distance between the R130 guanidinium side chain and the backbone carboxyl oxygen of L510 is 3.3 Å. (D) Superimposition of the modeled PapB−PapA complex onto the BlrP1 crystal structure (gray). The PapB monomers are colored magenta and green and the PapA monomers blue and yellow.

α+β sandwich with the flavin flanked by the two long α-helices (Figure 5A). The positions of two C-terminal α-helices are parallel to the β-sheet, which is a structural feature found for the BlrP1 BLUF domain (*38*, *53*). For other BLUF domains (*54*−*60*), the two C-terminal α-helices are oriented perpendicular to the β-sheet. The model of the EAL domain of PapA (residues 298−558) was constructed using the EAL domain of BlrP1 (residues 143−400) as the template. The docking simulation was then performed with ZDOCK (*49*), and we obtained several possible structures (Figure 2 of the Supporting Information). Figure 5B shows the best structure for PapB bound to the PapA EAL domain. The PapB C-terminal α-helices interacted with the connector region between the two EAL surfaces that form the interface. The docked PapB−PapA structure was superimposed on the crystal structure of BlrP1 (Figure 5D). Although the sequence identities between the BlrP1 and PapB BLUF domains and the BlrP1 and PapA EAL domains are each only ~20% (Figure 3 of the Supporting Information), the superimposition was good (root-mean-square deviation value of 6.42 Å). Notably, we did not need to refer to the BlrP1 structure to dock PapA and PapB.

We next tested experimentally whether the docked structure was a true representation of the PapA−PapB complex. Specifically, in the docked complex, the PapB Arg130 side chain and the PapA Leu510 backbone carboxyl oxygen are within hydrogen bonding distance (Figure 5C). The corresponding amino acids are conserved in the EAL domains of PapA and BlrP1, and in the BLUF domains of PapB and BlrP1 (Figure 3 of the Supporting Information). Furthermore, a similar orientation of the residues is present in the BlrP1 crystal structure (*38*), which suggests that these residues help stabilize the domain−domain interaction. We assessed the role of this possible hydrogen bond by site-directed mutagenesis. First, Arg130 of PapB was mutated to Ala, and the ability of the mutant (R130A) to bind PapA was characterized. As shown in Figure 4A, R130A bound poorly to PapA, which indicated that Arg130 is necessary for a strong interaction with PapA. We also analyzed the role of Leu510 of PapA by mutating it to Ala. As shown in Figure 4B, the mutation did not alter the ability of PapA to bind to PapB.

We next recorded the decay kinetics of the R130A photocycle after illumination. The dark and light absorption spectra of R130A were identical to those of WT PapB (data not shown). However, the decay kinetics of light-activated R130A was very different from that of WT. Specifically, the light-induced spectrum of R130A decayed biphasically; the half-times for the first and second phases at pH 8.0 were ~6 and ~3 s, respectively [Figure 2B (■)]. Addition of an equimolar amount of PapA slightly accelerated the rate at which R130A decayed to the dark state [Figure 2B (▲)], although the effect was weaker than that observed for WT (Figure 2A).

Analyses of the Effects of PapA and PapB on Biofilm Formation. Our in vitro analyses indicated that PapA functions as a phosphodiesterase that degrades c-di-GMP and that PapB, in response to blue light, enhances PapA activity. To assess the effects these proteins have on biofilm formation, we constructed *R. palustris* knockout mutants that lacked PapA (Δ*papA*), PapB (Δ*papB*), or both proteins (Δ*papA*Δ*papB*) and characterized their phenotypes. We determined the effects of blue light irradiation on the abilities of the WT and mutated strains to form biofilms, because the levels of cellular c-di-GMP control biofilm formation in some bacterial species (*1*−*5*), although this ability had not been reported previously for *R. palustris*. In the dark, the WT and mutated strains did not form significant biofilms (Figure 6A). Conversely, when illuminated with blue light (λ_{max} = 450 nm), the WT and all mutated strains enhanced biofilm formation (Figure 6A,B). Quantitative analysis indicated that the levels of biofilm formation of Δ*papB* and Δ*papA*Δ*papB* under high-blue light conditions (250 μmol m^{-2} s^{-1}) were significantly higher than those observed for WT (Figure 6B). Thus, PapB inhibited biofilm formation in response to the high intensity of blue light. The Δ*papA* mutant also enhanced biofilm formation by blue light illumination; however, the extent of biofilm formation under high-blue light conditions was less than that observed for Δ*papB* and Δ*papA*Δ*papB* (Figure 6B).

DISCUSSION

c-di-GMP is an important second messenger for a wide variety of physiological processes in bacteria (*1*−*8*). Although the enzymes responsible for the synthesis and hydrolysis of c-di-GMP have been well characterized, regulation of their activities is poorly understood. For the study reported here, we found that the blue light sensor protein PapB enhances the c-di-GMP hydrolysis activity of PapA, both of which are from the purple photosynthetic bacterium *R. palustris*. We also showed that this regulation is crucial for blue light-dependent control of biofilm formation by this bacterium. This is the first report correlating a physiological function with c-di-GMP degradation induced by blue light.

Recently, the crystal structure of the dimeric BLUF protein, BlrP1, was reported (*38*). BlrP1 is a photoactivated phosphodiesterase that has one BLUF and one EAL domain per subunit. An examination of the BlrP1 structure suggested that the light signal is transferred from its BLUF to its EAL domain by a conformational change at the BLUF domain−EAL domain interface that involves the BLUF domain C-terminal helices of one monomer, the connector region between the EAL−EAL interface, and the β-strands of the EAL domains. This conformational

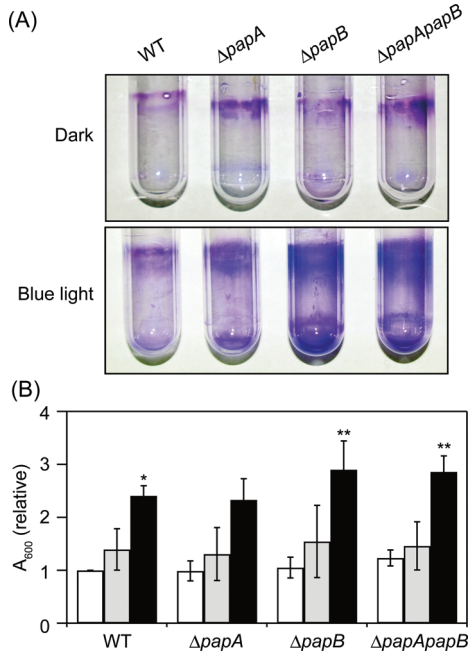

FIGURE 6: Biofilm formation by the *R. palustris* WT, Δ*papA*, Δ*papB*, and Δ*papApapB* strains. (A) Cells were grown statically for 70 h at room temperature (~24 °C) in the dark or under blue light (λ_{max} = 470 nm, 250 μmol m^{-2} s^{-1}). Biofilm formation was visualized by crystal violet staining. (B) Crystal violet staining was quantified from four independent experiments. White, gray, and black bars are for cells grown in the dark, under low blue light (50 μmol m^{-2} s^{-1}), and under high blue light (250 μmol m^{-2} s^{-1}), respectively. The value for WT grown in the dark was set to 1.0 in each measurement. Error bars represent the standard deviation of four replications. *$P < 0.01$ in a Student's *t*-test compared with values for WT grown in the dark. **$P < 0.01$ in a Student's *t*-test compared with values for WT grown under high-blue light conditions.

change may be a general feature of the activation of phosphodiesterase activities of EAL domains (*38*). We showed by a docking simulation and by biochemical analyses that the PapA EAL domain and the PapB BLUF domain bind in a manner similar to that of the corresponding BlrP1 domains (Figure 5D), which suggests that the light-dependent activation mechanism is conserved in BlrP1 and the PapA−PapB complex, although the BLUF domain−EAL domain complex is an intramolecular one in BlrP1 and an intermolecular one in the PapA−PapB complex. The intermolecular PapA−PapB complex lends itself as a model for biochemical analyses of BLUF domain−EAL domain interactions. In the model PapA−PapB complex, there appears to be a hydrogen bond between Leu510 of PapA and Arg130 of PapB (Figure 5C). This interaction is also seen in the BlrP1 crystal structure (*38*). The R130A mutation in PapB reduced the strength of the interaction (Figure 4A), which suggested that the R130 side chain helps maintain the PapB−PapA complex. In contrast, the PapA L510A mutant bound PapB with an affinity similar to that of WT PapA (Figure 4B). Given the fact that the predicted interaction between Arg130 and Leu510 involves the latter's backbone carboxyl oxygen (Figure 5C), it appears that the side chain of Leu510 itself does not influence the PapA−PapB interaction.

PapB is a small protein (~15 kDa) that contains a single BLUF domain. Spectroscopic analyses indicated that it shows a typical BLUF domain photocycle; illumination caused a red shift in the flavin absorption, which decayed to the ground state in the dark (Figure 1). This cycle is similar to that of the BLUF protein PixD/Slr1694 from the cyanobacterium *Synechocystis* sp. PCC6803. PixD contains a single BLUF domain and functionally interacts with the putative transcription factor, PixE (*31*, *32*, *36*). Previous studies indicated that PixD associates with PixE in a light-dependent manner such that dark-adapted PixD makes a complex with PixE, and subsequent illumination causes the complex to dissociate (*36*, *61*). In vivo analysis indicated that this interaction is crucial for the light-dependent cell motility of this cyanobacterium (*36*). Thus, this protein−protein interaction itself is important for the transfer of the blue light signal from PixD to PixE. We showed that PapB also directly interacts with its partner protein, PapA (Figure 4). However, in this case, the interaction is not light-dependent; PapB binds PapA under both dark and light conditions (Figure 4). In fact, in the dark, the c-di-GMP hydrolysis activity of PapA is not influenced by the addition of PapB; PapB enhances PapA activity only when it is exposed to light (Table 1). These results indicated that the initial PapA−PapB complex does not control PapA activity in response to blue light. Thus, among BLUF domains, there are at least two distinct mechanisms for transferring the blue light signal to downstream regions; one is through a light-dependent interaction (as shown for the PixD−PixE complex), and the other occurs by modulating the conformation of the complex (as shown for the PapB−PapA complex). For the latter, complex formation is necessary, but not sufficient, for the transduction of the light signal; a conformational change is also required by the light-activated PapB.

Two types of BLUF domain conformations have been characterized. For one, the two C-terminal α-helices are oriented perpendicular to the β-sheet, e.g., in the structure of PixD (*60*). For the other, the two C-terminal α-helices are oriented parallel to the β-sheet, e.g., in BlrP1 (*38*, *53*). The different orientations of the C-terminal α-helices may specify which output domain(s) binds to a given BLUF domain. We propose that the two types of BLUF domains have distinct mechanisms for blue light signal transduction: one occurs via a light-dependent protein−protein dissociation and the other via a conformational modulation of the complex that does not require a light-dependent dissociation step. These different mechanisms may reflect the coevolution of the BLUF domain C-terminal α-helices and output module for transduction of a blue light signal that controls a specific physiological activity.

For *R. palustris*, the light-dependent control of biofilm formation via the modulation of the c-di-GMP level may be complex. The WT and all mutant strains tested enhanced biofilm formation by blue light (Figure 6). It has been established that c-di-GMP positively regulates biofilm formation (*1*−*5*). This suggests that in *R. palustris*, an unidentified blue light sensor protein(s), other than PapB, positively regulates c-di-GMP synthesis and biofilm formation. However, under high-blue light conditions, Δ*papB* and Δ*papApapB* show enhanced biofilm formation compared to that observed in WT (Figure 6B), suggesting that PapB negatively and dominantly controls biofilm formation in response to the high intensity of blue light by activating c-di-GMP hydrolysis activity. Such a complex regulatory mechanism involving multiple blue light input cascades may be needed to increase the dynamic range of the light sensitivity and thereby fine-tune the control of biofilm formation. Because the extent of Δ*papA* biofilm formation under high-blue light conditions was lower than that of Δ*papB* and Δ*papApapB* (Figure 6B), PapB may also functionally interact with other c-di-GMP phosphodiesterases to reduce cellular c-di-GMP levels under high-blue light conditions. Notably, the *R. palustris*

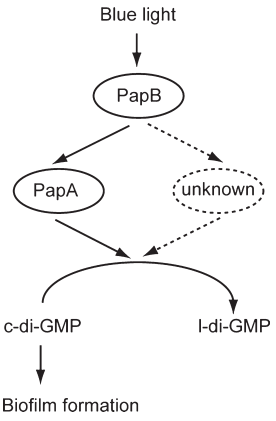

FIGURE 7: Model for blue light-dependent biofilm formation by PapB in *R. palustris*. Blue light-activated PapB enhances PapA phosphodiesterase activity. PapB may also functionally interact with other unidentified EAL domain proteins to decrease the level of cellular c-di-GMP under blue light conditions.

genome contains more than 15 genes that encode enzymes containing EAL domains. Our proposed pathway for modulating the c-di-GMP levels is illustrated in Figure 7, which illustrates how the blue light signal is transferred from PapB to c-di-GMP phosphodiesterases for controlling c-di-GMP degradation.

In summary, we characterized the transduction of the blue light signal via the intermolecular interaction between the BLUF domain of PapB and the EAL domain of PapA, which revealed how the signal is transferred from the light-activated BLUF domain to its downstream component. A more detailed understanding of the PapA−PapB interaction might find use in a method that allows the artificial control of cellular c-di-GMP levels by BLUF proteins.

SUPPORTING INFORMATION AVAILABLE

Physical and genetic map of the *papA* and *papB* region in the *R. palustris* genome, results of protein docking calculations of PapA and PapB, and amino acid sequence alignments of EAL domains of PapA and BlrP1 as well as BLUF domains of BlrP1 and PapB. This material is available free of charge via the Internet at http://pubs.acs.org.

REFERENCES

1. Romling, U., and Amikam, D. (2006) Cyclic di-GMP as a second messenger. *Curr. Opin. Microbiol. 9*, 218–228.
2. Tamayo, R., Pratt, J. T., and Camilli, A. (2007) Roles of cyclic diguanylate in the regulation of bacterial pathogenesis. *Annu. Rev. Microbiol. 61*, 131–148.
3. Jenal, U., and Malone, J. (2006) Mechanisms of cyclic-di-GMP signaling in bacteria. *Annu. Rev. Genet. 40*, 385–407.
4. Wolfe, A. J., and Visick, K. L. (2008) Get the message out: Cyclic-di-GMP regulates multiple levels of flagellum-based motility. *J. Bacteriol. 190*, 463–475.
5. Hengge, R. (2009) Principles of c-di-GMP signalling in bacteria. *Nat. Rev. Microbiol. 7*, 263–273.
6. Ross, P., Weinhouse, H., Aloni, Y., Michaeli, D., Weinberger-Ohana, P., Mayer, R., Braun, S., de Vroom, E., van der Marel, G. A., van Boom, J. H., and Benziman, M. (1987) Regulation of cellulose synthesis in *Acetobacter xylinum* by cyclic diguanylic acid. *Nature 325*, 279–281.
7. Kumar, M., and Chatterji, D. (2008) Cyclic di-GMP: A second messenger required for long-term survival, but not for biofilm formation, in *Mycobacterium smegmatis*. *Microbiology 154*, 2942–2955.
8. Duerig, A., Abel, S., Folcher, M., Nicollier, M., Schwede, T., Amiot, N., Giese, B., and Jenal, U. (2009) Second messenger-mediated spatiotemporal control of protein degradation regulates bacterial cell cycle progression. *Genes Dev. 23*, 93–104.
9. Fang, X., and Gomelsky, M. (2010) A post-translational, c-di-GMP-dependent mechanism regulating flagellar motility. *Mol. Microbiol. 76*, 1295–1305.
10. Paul, K., Nieto, V., Carlquist, W. C., Blair, D. F., and Harshey, R. M. (2010) The c-di-GMP binding protein YcgR controls flagellar motor direction and speed to affect chemotaxis by a "backstop brake" mechanism. *Mol. Cell 38*, 128–139.
11. Boehm, A., Kaiser, M., Li, H., Spangler, C., Kasper, C. A., Ackermann, M., Kaever, V., Sourjik, V., Roth, V., and Jenal, U. (2010) Second messenger-mediated adjustment of bacterial swimming velocity. *Cell 141*, 107–116.
12. Tamayo, R., Tischler, A. D., and Camilli, A. (2005) The EAL domain protein VieA is a cyclic diguanylate phosphodiesterase. *J. Biol. Chem. 280*, 33324–33330.
13. Galperin, M. Y., Nikolskaya, A. N., and Koonin, E. V. (2001) Novel domains of the prokaryotic two-component signal transduction systems. *FEMS Microbiol. Lett. 203*, 11–21.
14. Galperin, M. Y. (2004) Bacterial signal transduction network in a genomic perspective. *Environ. Microbiol. 6*, 552–567.
15. Schmidt, A. J., Ryjenkov, D. A., and Gomelsky, M. (2005) The ubiquitous protein domain EAL is a cyclic diguanylate-specific phosphodiesterase: Enzymatically active and inactive EAL domains. *J. Bacteriol. 187*, 4774–4781.
16. Ryjenkov, D. A., Tarutina, M., Moskvin, O. V., and Gomelsky, M. (2005) Cyclic diguanylate is a ubiquitous signaling molecule in bacteria: Insights into biochemistry of the GGDEF protein domain. *J. Bacteriol. 187*, 1792–1798.
17. Amikam, D., and Galperin, M. Y. (2006) PilZ domain is part of the bacterial c-di-GMP binding protein. *Bioinformatics 22*, 3–6.
18. Ryjenkov, D. A., Simm, R., Romling, U., and Gomelsky, M. (2006) The PilZ domain is a receptor for the second messenger c-di-GMP: The PilZ domain protein YcgR controls motility in enterobacteria. *J. Biol. Chem. 281*, 30310–30314.
19. Sudarsan, N., Lee, E. R., Weinberg, Z., Moy, R. H., Kim, J. N., Link, K. H., and Breaker, R. R. (2008) Riboswitches in eubacteria sense the second messenger cyclic di-GMP. *Science 321*, 411–413.
20. Lee, E. R., Baker, J. L., Weinberg, Z., Sudarsan, N., and Breaker, R. R. (2010) An allosteric self-splicing ribozyme triggered by a bacterial second messenger. *Science 329*, 845–848.
21. Smith, K. D., Lipchock, S. V., Livingston, A. L., Shanahan, C. A., and Strobel, S. A. (2010) Structural and biochemical determinants of ligand binding by the c-di-GMP riboswitch. *Biochemistry 49*, 7351–7359.
22. Smith, K. D., Lipchock, S. V., Ames, T. D., Wang, J., Breaker, R. R., and Strobel, S. A. (2009) Structural basis of ligand binding by a c-di-GMP riboswitch. *Nat. Struct. Mol. Biol. 16*, 1218–1223.
23. van der Horst, M. A., and Hellingwerf, K. J. (2004) Photoreceptor proteins, "star actors of modern times": A review of the functional dynamics in the structure of representative members of six different photoreceptor families. *Acc. Chem. Res. 37*, 13–20.
24. Möglich, A., Yang, X., Ayers, R. A., and Moffat, K. (2010) Structure and function of plant photoreceptors. *Annu. Rev. Plant Biol. 61*, 21–47.
25. Gomelsky, M., and Klug, G. (2002) BLUF: A novel FAD-binding domain involved in sensory transduction in microorganisms. *Trends Biochem. Sci. 27*, 497–500.
26. Masuda, S., and Bauer, C. E. (2005) The antirepressor AppA uses the novel flavin-binding BLUF domain as blue-light-absorbing photoreceptor to control photosystem synthesis. In Handbook of Photosensory Receptors (Briggs, W. R., and Spudich, J., Eds.) p 443, Wiley-VCH Verlag GmbH, Weinheim, Germany.
27. Masuda, S., and Bauer, C. E. (2002) AppA is a blue light photoreceptor that antirepresses photosynthesis gene expression in *Rhodobacter sphaeroides*. *Cell 110*, 613–623.
28. Gomelsky, M., and Kaplan, S. (1995) *appA*, a novel gene encoding a trans-acting factor involved in the regulation of photosynthesis gene expression in *Rhodobacter sphaeroides* 2.4.1. *J. Bacteriol. 177*, 4609–4618.
29. Braatsch, S., Gomelsky, M., Kuphal, S., and Klug, G. (2002) A single flavoprotein, AppA, integrates both redox and light signals in *Rhodobacter sphaeroides*. *Mol. Microbiol. 45*, 827–836.
30. Masuda, S., and Ono, T. A. (2005) Adenylyl cyclase activity of Cya1 from the cyanobacterium *Synechocystis* sp. strain PCC 6803 is inhibited by bicarbonate. *J. Bacteriol. 187*, 5032–5035.
31. Masuda, S., Hasegawa, K., Ishii, A., and Ono, T. A. (2004) Light-induced structural changes in a putative blue-light receptor with a novel FAD binding fold sensor of blue-light using FAD (BLUF); Slr1694 of *Synechocystis* sp. PCC6803. *Biochemistry 43*, 5304–5313.

32. Okajima, K., Yoshihara, S., Fukushima, Y., Geng, X., Katayama, M., Higashi, S., Watanabe, M., Sato, S., Tabata, S., Shibata, Y., Itoh, S., and Ikeuchi, M. (2005) Biochemical and functional characterization of BLUF-type flavin-binding proteins of two species of cyanobacteria. *J. Biochem. 137*, 741–750.
33. Rajagopal, S., Key, J. M., Purcell, E. B., Boerema, D. J., and Moffat, K. (2004) Purification and initial characterization of a putative blue light-regulated phosphodiesterase from *Escherichia coli*. *Photochem. Photobiol. 80*, 542–547.
34. Tschowri, N., Busse, S., and Hengge, R. (2009) The BLUF-EAL protein YcgF acts as a direct anti-repressor in a blue-light response of *Escherichia coli*. *Genes Dev. 23*, 522–534.
35. Hasegawa, K., Masuda, S., and Ono, T. A. (2006) Light induced structural changes of a full-length protein and its BLUF domain in YcgF(Blrp), a blue-light sensing protein that uses FAD (BLUF). *Biochemistry 45*, 3785–3793.
36. Masuda, S., Hasegawa, K., Ohta, H., and Ono, T. A. (2008) Crucial role in light signal transduction for the conserved Met93 of the BLUF protein PixD/Slr1694. *Plant Cell Physiol. 49*, 1600–1606.
37. Iseki, M., Matsunaga, S., Murakami, A., Ohno, K., Shiga, K., Yoshida, K., Sugai, M., Takahashi, T., Hori, T., and Watanabe, M. (2002) A blue-light-activated adenylyl cyclase mediates photoavoidance in *Euglena gracilis*. *Nature 415*, 1047–1051.
38. Barends, T. R., Hartmann, E., Griese, J. J., Beitlich, T., Kirienko, N. V., Ryjenkov, D. A., Reinstein, J., Shoeman, R. L., Gomelsky, M., and Schlichting, I. (2009) Structure and mechanism of a bacterial light-regulated cyclic nucleotide phosphodiesterase. *Nature 459*, 1015–1018.
39. Purcell, E. B., Siegal-Gaskins, D., Rawling, D. C., Fiebig, A., and Crosson, S. (2007) A photosensory two-component system regulates bacterial cell attachment. *Proc. Natl. Acad. Sci. U.S.A. 104*, 18241–18246.
40. van der Horst, M. A., Stalcup, T. P., Kaledhonkar, S. K., Kumauchi, M., Hara, M., Xie, A., Hellingwerf, K. J., and Hoff, W. D. (2009) Locked chromophore analogs reveal that photoactive yellow protein regulates biofilm formation in the deep sea bacterium *Idiomarina loihiensis*. *J. Am. Chem. Soc. 131*, 17443–17451.
41. Laan, W., Bednarz, T., Heberle, J., and Hellingwerf, K. J. (2004) Chromophore composition of a heterologously expressed BLUF-domain. *Photochem. Photobiol. Sci. 3*, 1011–1016.
42. Hyodo, M., and Hayakawa, Y. (2004) An improved method for synthesis of cyclic bis(3′-5′)diguanylic acid (c-di-GMP). *Bull. Chem. Soc. Jpn. 77*, 2089–2093.
43. Schuck, P. (2000) Size-distribution analysis of macromolecules by sedimentation velocity ultracentrifugation and Lamm equation modeling. *Biophys. J. 78*, 1606–1619.
44. Masuda, S., and Bauer, C. E. (2004) Null mutation of HvrA compensates for loss of an essential *relA*/*spoT*-like gene in *Rhodobacter capsulatus*. *J. Bacteriol. 186*, 235–239.
45. Alexeyev, M. F. (1995) Three kanamycin resistance gene cassettes with different polylinkers. *BioTechniques 18*, 52, 54, 56.
46. Penfold, R. J., and Pemberton, J. M. (1992) An improved suicide vector for construction of chromosomal insertion mutations in bacteria. *Gene 118*, 145–146.
47. Larkin, M. A., Blackshields, G., Brown, N. P., Chenna, R., McGettigan, P. A., McWilliam, H., Valentin, F., Wallace, I. M., Wilm, A., Lopez, R., Thompson, J. D., Gibson, T. J., and Higgins, D. G. (2007) Clustal W and Clustal X version 2.0. *Bioinformatics 23*, 2947–2948.
48. Tsuji, M. (2010) Homology modeling for hyperchem, revision E1, Saitama, Japan.
49. Wiehe, K., Pierce, B., Tong, W. W., Hwang, H., Mintseris, J., and Weng, Z. (2007) The performance of ZDOCK and ZRANK in rounds 6−11 of CAPRI. *Proteins 69*, 719–725.
50. Lovell, S. C., Davis, I. W., Arendall, W. B., III, de Bakker, P. I. W., Word, J. M., Prisant, M. G., Richardson, J. S., and Richardson, D. C. (2003) *Proteins: Struct., Funct., Genet. 50*, 437–450.
51. Christen, M., Christen, B., Folcher, M., Schauerte, A., and Jenal, U. (2005) Identification and characterization of a cyclic di-GMP-specific phosphodiesterase and its allosteric control by GTP. *J. Biol. Chem. 280*, 30829–30837.
52. Dam, J., and Schuck, P. (2005) Sedimentation velocity analysis of heterogeneous protein-protein interactions: Sedimentation coefficient distributions *c*(*s*) and asymptotic boundary profiles from Gilbert-Jenkins theory. *Biophys. J. 89*, 651–666.
53. Wu, Q., and Gardner, K. H. (2009) Structure and insight into blue light-induced changes in the BlrP1 BLUF domain. *Biochemistry 48*, 2620–2629.
54. Jung, A., Domratcheva, T., Tarutina, M., Wu, Q., Ko, W. H., Shoeman, R. L., Gomelsky, M., Gardner, K. H., and Schlichting, I. (2005) Structure of a bacterial BLUF photoreceptor: Insights into blue light-mediated signal transduction. *Proc. Natl. Acad. Sci. U.S.A. 102*, 12350–12355.
55. Kita, A., Okajima, K., Morimoto, Y., Ikeuchi, M., and Miki, K. (2005) Structure of a cyanobacterial BLUF protein, Tll0078, containing a novel FAD-binding blue light sensor domain. *J. Mol. Biol. 349*, 1–9.
56. Grinstead, J. S., Hsu, S. T., Laan, W., Bonvin, A. M., Hellingwerf, K. J., Boelens, R., and Kaptein, R. (2006) The solution structure of the AppA BLUF domain: Insight into the mechanism of light-induced signaling. *ChemBioChem 7*, 187–193.
57. Anderson, S., Dragnea, V., Masuda, S., Ybe, J., Moffat, K., and Bauer, C. (2005) Structure of a novel photoreceptor, the BLUF domain of AppA from *Rhodobacter sphaeroides*. *Biochemistry 44*, 7998–8005.
58. Wu, Q., Ko, W. H., and Gardner, K. H. (2008) Structural requirements for key residues and auxiliary portions of a BLUF domain. *Biochemistry 47*, 10271–10280.
59. Jung, A., Reinstein, J., Domratcheva, T., Shoeman, R. L., and Schlichting, I. (2006) Crystal structures of the AppA BLUF domain photoreceptor provide insights into blue light-mediated signal transduction. *J. Mol. Biol. 362*, 717–732.
60. Yuan, H., Anderson, S., Masuda, S., Dragnea, V., Moffat, K., and Bauer, C. (2006) Crystal structures of the *Synechocystis* photoreceptor Slr1694 reveal distinct structural states related to signaling. *Biochemistry 45*, 12687–12694.
61. Yuan, H., and Bauer, C. E. (2008) PixE promotes dark oligomerization of the BLUF photoreceptor PixD. *Proc. Natl. Acad. Sci. U.S.A. 105*, 11715–11719.